Electronic Supplementary Material (ESI) for Nanoscale.

Supplementary Information

Bridge percolation: electrical connectivity of discontinued conducting slabs by metallic nanowires

A. Baret[1]*, L. Bardet[2], D. Oser, D. P. Langley, F. Balty[1], D. Bellet[2], N. D. Nguyen[1]

[1] *Department of Physics, CESAM / SPIN, University of Liège, Allée du Six Août 19, Liège B-4000, Belgium*

[2] *Univ. Grenoble Alpes, CNRS, Grenoble INP, LMGP, Grenoble F-38016, France*

*abaret@uliege.be

1. Microscope images of real samples of cracked ITO coated with sparse network

Figure S1 shows images of genuine cracked ITO samples obtained by scanning electron microscopy. They illustrate the particular fracture mechanism mentioned in the main manuscript, leading to an array of parallel defect lines (Fig. S1a). The concept of bridge percolation is materialized in Fig. S1b, which shows the connection of two adjacent parts of the ITO film (separated by a fracture line) by an individual Ag nanowire.

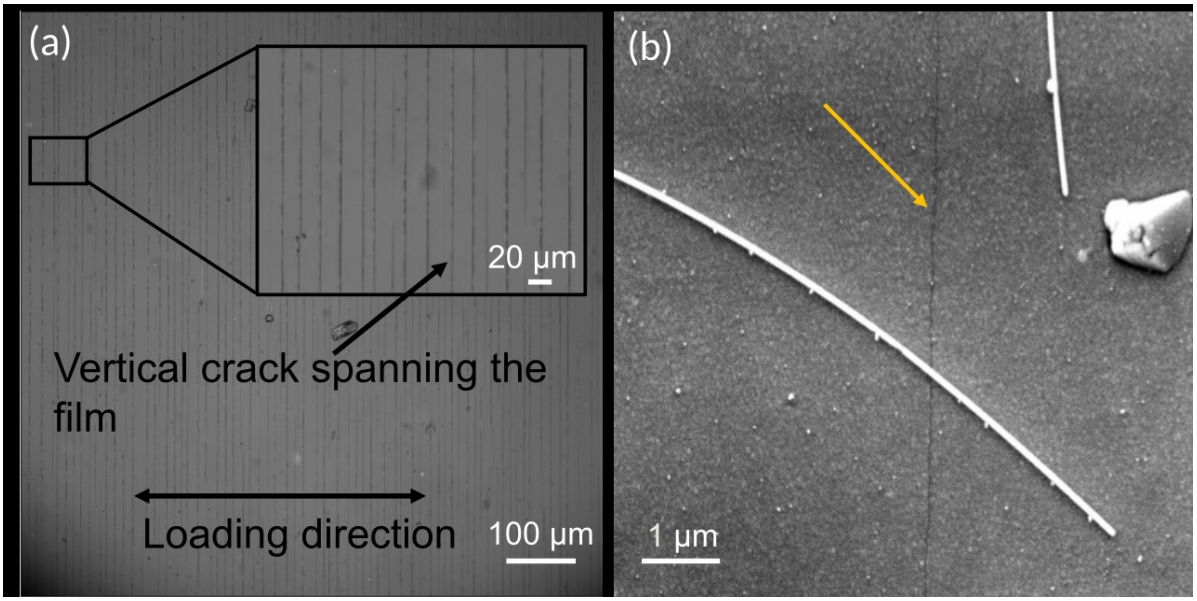

Figure S1. *(a) Optical image of cracks in a 150 nm thick ITO film deposited on a 0.175 mm thick PET substrate. (b) Scanning electron microscope image of a nanowire bridging a crack in an ITO film (highlighted by the yellow arrow).*

2. Percolation model

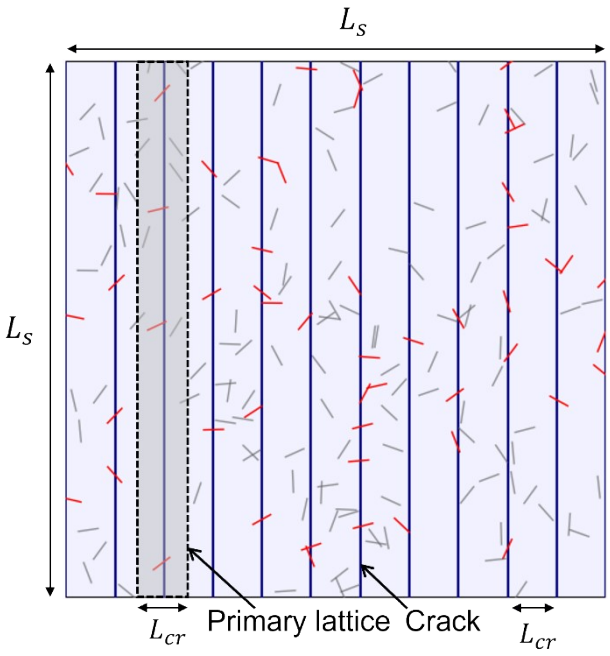

Figure S2. *Schematic network of parallel cracks (in blue) separated by a distance* L_{cr}*. A primary lattice is shown in dashed lines. The NWs are represented in red if they are bridging a crack, in grey otherwise.*

First, let us explicitly show that the average projected length of the nanowires, $\bar{L}_p$, is equal to $\frac{2L_{NW}}{\pi}$.

From Fig. 2, we can express the projected length of a single NW as a function of its angle θ with respect to the horizontal axis:

$$L_p(\theta) = \begin{cases} L_{NW}\cos(\theta) \; if \; \theta \in [0, \frac{\pi}{2}] \\ -L_{NW}\cos(\theta) \; if \; \theta \in [\frac{\pi}{2}, \pi] \end{cases}$$

As a consequence, considering a uniform angular distribution probability ($p(\theta) = \frac{1}{\pi}$)

$$\bar{L}_p(\theta) = \int_0^{\frac{\pi}{2}} \frac{L_{NW}\cos(\theta)}{\pi} d\theta + \int_{\frac{\pi}{2}}^{\pi} -\frac{L_{NW}\cos(\theta)}{\pi} d\theta$$

$$= \frac{L_{NW}}{\pi}[\sin(\theta)]_0^{\pi/2} - [\sin(\theta)]_{\pi/2}^{\pi} = \frac{L_{NW}}{\pi}[1-(-1)] = \frac{2L_{NW}}{\pi} \blacksquare$$

We also claim that the probability that a NW randomly deposited in a primary lattice (defined in the manuscript) is equal to $\bar{L}_p/L_{cr}$, where L_{cr} is the intercracks distance. An intuitive manner to visualize this result consists in picturing that a NW in a primary lattice can be located in L_{cr} specific x positions on this lattice, but only L_p of those possess an intersection point with the crack. This stems from the

fact that the NW can only have 1 or 0 intersection with the crack. Finally, let us show how we can derive equation (8) and (9) from the manuscript using Eq. (7) from the manuscript.

We start with Eq. (7):

$$P(N_{NW}) = \left(1 - \left(1 - \frac{1}{N_{cr}L_{cr}}\bar{L}_p\right)^{N_{NW}}\right)^{N_{cr}}.$$

Given that N_{NW}^{C} is defined as $P\left(N_{NW}^{C}\right) = 1/2$, we have

$$\frac{1}{2} = \left(1 - \left(1 - \frac{1}{N_{cr}L_{cr}}\bar{L}_p\right)^{N_{NW}^{C}}\right)^{N_{cr}}.$$

As a consequence, since $0.5 > 0$,

$$2^{-1/N_{cr}} = 1 - \left(1 - \frac{1}{N_{cr}L_{cr}}\bar{L}_p\right)^{N_{NW}^{C}}$$

$$1 - 2^{-1/N_{cr}} = \left(1 - \frac{1}{N_{cr}L_{cr}}\bar{L}_p\right)^{N_{NW}^{C}}$$

$$N_{NW}^{C}\ln\left(1 - \frac{1}{N_{cr}L_{cr}}\bar{L}_p\right) = ln(1 - 2^{-1/N_{cr}})$$

$$N_{NW}^{C} = \frac{ln(1 - 2^{-1/N_{cr}})}{ln(1 - \frac{\bar{L}_p}{N_{cr}L_{cr}})} \blacksquare$$

In order to get Eq. (9), we use the approximation that $\bar{L}_p \ll L_s \approx N_{cr}L_{cr}$, and thus we have a factor of the form

$$\ln(1 - x), where\ x = \frac{\bar{L}_p}{N_{cr}L_{cr}} \ll 1.$$

We use the well-known Taylor expansion of the function $\ln(1 + x) = x + O(x^2)$, such that, in the first order approximation, we have

$$\ln\left(1 - \frac{\bar{L}_p}{N_{cr}L_{cr}}\right) \approx -\frac{\bar{L}_p}{N_{cr}L_{cr}} \approx -\frac{\bar{L}_p}{L_s} \blacksquare$$

3. Percolation results

3.1 On the influence of L_s on the critical density

In the manuscript, Fig. 4b shows that amd_c explicitly depends on L_s, and we claim that it is a consequence to "the intrinsinc directional anisotropy of the system due to the uniaxial parallel cracks in the sample". This can be understood as follows.

Since the parallel cracks are all aligned in the same direction and fully span the substrate from top to bottom, the vertical direction does not play any role in the conduction phenomenon. In standard percolation, increasing L_s by a factor α has two countering effects. On the one hand, the system's area is scaled by a factor α^2. On the other hand, since the wires are randomly distributed, the required number to reach percolation will also be increased by α^2. Intuitively, this can be understood by recognizing that "α more" NWs will be required to span the sample in the facing electrodes direction but the probability that a NW participates in a cluster in this particular direction is scaled by 1/α. Consequently, in conventional percolation, amd_c scales as α^2/α^2 and is thus scale-invariant. In the case of bridge percolation however, since the location of a NW in the direction parallel to the cracks does not have any impact on its bridging probability, the same reasoning leads to the result that the percolation probability is only scaled by α, such that amd_c depends linearly on L_s.

3.2 Additional results from the model

The evolution of the critical amd as a function of the system's parameters provides a broader range of interesting features to be discussed. As a reminder, in our manuscript (Eq. 8), we show

$$amd_c = -\frac{m}{L_s}\frac{\ln\left(1-2^{-\frac{L_{cr}}{L_s}}\right)}{\bar{L}_p}.$$

It should be noted here that the critical amd proves to be independent on $\bar{L}_p$. This surprising and counter-intuitive observation can be explained by the fact that while using NWs of size αL_{NW} reduces n_c by a factor α, it also implies that the NWs have a mass α times higher than their initial one. In other words, using wires that are, for instance, twice as long, is equivalent, in terms of mass, to using twice the number of NWs. This result highlights the utility of the amd as a density quantifier, as the industry is most interested in the quantity of raw material required than by the theoretical number of NWs to deposit. This independence is also validated by the MC simulations outcome, shown in Fig. S3, and resonates with M. Lagrange's findings in her PhD thesis[1].

[1] 1 M. Lagrange, PhD thesis, Université Grenoble Alpes, 2015.

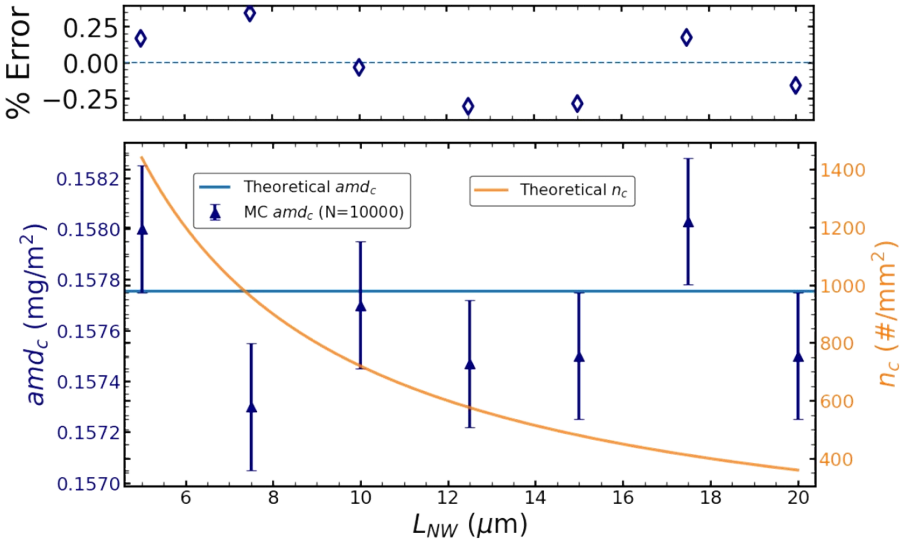

Figure S3. *Evolution of the critical* amd *as a function of the NWs length, with system size* L_s*= 500 µm and* L_{cr}*= 20 µm. As predicted by the analytical approach, MC results are constant with respect to changes in* L_{NW}*. Note the particularly zoomed scale for* amd_c*. The theoretical evolution of the critical density of NWs is also shown in orange on the right vertical axis, to highlight its predicted decrease with increasing NWs length. The error (expressed in %) is shown in the top graph, which displays the quality of the agreement between the analytical prediction and MC results.*

4. Conductivity model

In this section, we would like to describe more comprehensively the model used to calculate the conductivity of the hybrid systems presented in our manuscript.

The first step consists in taking into account the non-infinite resistance of the cracks. As described in the manuscript, it is known that the finite resistance originates from the leftover material at the

bottom of the cracks. In order to account for this contribution to the conductivity of the system, we hypothesize that they constitute a parallel path for the current flow. In other words, the system is decoupled into two distinct subsystems: the ITO conducting sectors + bridging NWs on the one hand, and the bottom layer of conducting material on the other hand, as represented in Fig S4a. The sheet resistance of this bottom layer is by definition equal to the initial resistance (R_0) of the fractured ITO film as a whole. This hypothesis comes at a cost: it implies that the current flowing in the conducting material of the cracks is strictly different from that flowing in the upper part of the system. While quite strong, this assumption is supported by two important observations. First, the depth of the cracks represents a significant portion of the thickness of the ITO film. As a consequence, the current lines going through the conducting part of the cracks are constricted at the very bottom of the ITO film. Secondly, and perhaps most notably, the voltage bias is applied to the system through the lateral edges of the system. This induces a preferential in-plane direction for the current flow, which will thus favourably remain at the bottom of the ITO film. Moreover, this preferential flow direction is enhanced by the carrier mobility anisotropy of ITO: due to the particular arrangement of the orbitals in the ITO crystal, the conduction along the vertical axis can be as much as four orders of magnitude lower than that in the parallel direction (to the thin film plane). This decoupling step is illustrated in Fig S4a.

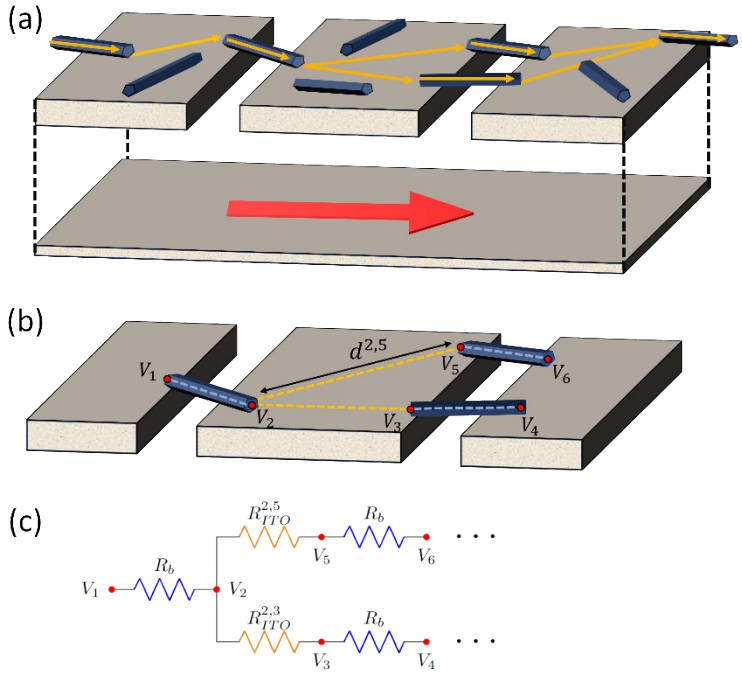

Figure S4. *(a) Model system decoupled into two distinct, independent subsystems. The current flowing in each of them is independent from the other. (b) identified voltage nodes and resistive elements and (c) equivalent electrical circuit representation.*

The second step in the model is dedicated to the modelling of the bridged ITO subsystem. In order to use the Multi-Nodal Representation paradigm, well-defined voltage nodes, or equivalently, resistive elements, need to be identified. In this model, each bridge acts as a resistor separating two voltage

nodes. Our first goal is to determine a value for the resistance of one single bridge R_b. As represented in Fig. S4b since the current must both enter and exit the bridging NWs, $R_b = R_{con} + R_{in} + R_{con} = 2R_{con} + R_{in}$, where R_{con} is the contact resistance between the ITO substrate and an Ag NW, and R_{in} is the inner wire resistance. To the best of our knowledge, there exists no report of the value of the contact resistance between an Ag NW and an ITO substrate in the literature. Even more surprisingly, this value does not seem reported for any thin metallic substrate-metallic NW contact. As a first approximation, however, the contact resistivity ρ_{con} for Ag/ITO plane interfaces is used to calculate the contact resistance. In general, the contact resistance between two films is given by $R_{con} = \rho_{con} A_{con}$ where A_c is the contact area. Borchert et al. have determined that, for Ag/ITO plane interfaces, $\rho_{con} = 2.4 \times 10^{-5}\ \Omega.cm^2$. Furthermore, given the pentagonal cross-section of the Ag NWs, the contact area A_{con} can be estimated by a simple geometrical development $A_{con} = w_{con} \times L_{con} = \frac{2D_{NW}}{1+\sqrt{5}} L_{con}$, where w_{con} and L_{con} are the width and length of the contact area, respectively. Thus, we obtain (in Ω)

$$R_{con} = \frac{2.4 \times 10^{-5}}{2D_{NW}L_{con}}(1+\sqrt{5}) = \frac{3.88 \times 10^{-5}}{D_{NW}L_{con}}.$$

As an illustration for the order of magnitude, in the case of 15 µm-long NWs of diameter 50 nm, and with the assumption that, in average, $L_{con} = \frac{L_{NW}}{2}$, we obtain $R_{con} = 11640\ \Omega$. In general, $R_{in} \approx 1\ \Omega$, such that it is negligible with respect to R_{con}. Consequently, R_b can be rewritten as $R_b \approx 2R_{con}$. Using the above-calculated value for R_{con}, R_b is thus of the order of 23000 Ω. This value can appear as rather high, but if a sufficiently high number N_b of NWs bridge the same crack, the overall resistance associated to the bridging of the crack scales as $\frac{1}{N_b}$.

It is important to note that conceptually, while the whole contact length is taken into account to calculate R_{con}, the current enters and exits the NWs from a specific location, which represents a unique voltage node in the circuit.

The last step needed to complete the electrical mapping of the system consists in considering the resistance associated to the ITO conducting slabs. As the current is free to spread across the conducting material, we are once again faced with the issue of having to discretize an inherently continuous physical phenomenon. In a first, simplified approach, we imagine that the whole set of current lines are constrained together, *i.e.* that they do not spread across the ITO film. The distance in the ITO substrate that the current must travel is defined as $d_{i,j}$, where i,j are the voltage nodes associated to the entry and end points of the current in the ITO sector, respectively. Furthermore, the individual current lines are assumed to be constrained to a channel of width D_{NW}, such that they do not spread after their injection into the conducting slab by the bridging NW.

A more complex quantity to evaluate is the cross-sectional area of the volume in which we imagine that the current lines are restricted. Two values can reasonably be used: either the cross-sectional area of the NWs, or the depth of the ITO thin film. As both are of the same order of magnitude, this choice does not have critical consequences. In the end, we decided that the depth of the ITO film was more relevant. Thus, the model assumes that the current goes from one side of an ITO sector to the

other through a channel of length $d_{i,j}$ and of rectangular cross-sectional area $t_{ITO} \times D_{NW}$, where t_{ITO} is the thickness of the ITO thin film. As a consequence, Pouillet's law yields

$$R_{ITO}^{i,j} = \frac{\rho_{ITO} d^{i,j}}{t_{ITO} D_{NW}}.$$

As mentioned earlier, this expression does not take into account the spreading of the current lines in the ITO substrate. In order to circumvent this problem, we take advantage of the π/ln2 factor acting as a geometrical correction to sheet resistance four-probe measurements, and that was explicitly designed to account for the spreading of the current in thin films. Note that this implies that the effective resistance associated to the ITO sectors is about 4 times higher than the one predicted by the naive use of Pouillet's law. As a consequence, if two bridge end-entry points are separated by a distance $d_{i,j}$, the resistance through the ITO layer between those two points is

$$R_{ITO}^{i,j} = \frac{\pi}{\ln(2)} \rho_{ITO} \frac{d^{i,j}}{t_{ITO} D_{NW}}.$$